The Hot Spot Hepatobiliary Scan in Focal Nodular Hyperplasia

Hatem Boulahdour, Daniel Cherqui, Frédéric Charlotte, Alain Rahmouni, Daniel Dhumeaux, Elie-Serge Zafrani and Michel Meignan

Departments of Nuclear Medicine, General Anatomy Pathology, Radiology, Hepatobiliary-Gastroenterology, Hôpital Henri Mondor, Université Paris XII-Val de Marne, Créteil, France

A prospective study was performed on 14 patients with histologically proven focal nodular hyperplasia (FNH) using a hepatobiliary scan with trimethylbromoimino-diacetic acid (TBIDA) and a colloid scan with rhenium sulfur colloids. TBIDA uptake was relatively normal in the region of the tumor, but during the clearance phase 23/25 of the tumors were detected by a hot spot of radioactivity. Depending on the relative contrast achieved between the tumor and normal liver, this hot spot appeared early or later, but was always present at 60 min. In three tumors, a "doughnut" pattern was observed within the hot spot due to a central defect. Hypervascularization was observed during the perfusion phase in 76% of the tumoral sites and normal colloid uptake in only 64%. The detectability of FNH appears greater with TBIDA (92%) than with CT or MRI (84%). The high prevalence of hot spots may be due to careful technological conditions when obtaining hepatobiliary scans. Late images, overexposed films, multiple views and stimulation of gallbladder excretion increased tumor detectability. The hot spot sign may be a useful tool when combined with the results of other imaging modalities in the diagnosis of FNH. The peculiar pathology of FNH with fibrosis, hyperplastic hepatocytes and cholangiolar proliferation might explain this scintigraphic appearance.

J Nucl Med 1993; 34:2105–2110

Focal nodular hyperplasia (FNH) is a benign tumor of the liver with an innocuous natural history. It is characterized pathologically by a cholangiolar proliferation associated with hyperplastic hepatocytes, blood vessels and fibrosis (*1*). FNH has been studied by various imaging techniques, i.e., ultrasonography (US), computed tomography (CT) and magnetic resonance imaging (MRI) (*2,3*).

Nuclear medicine tracers, including colloids and hepatobiliary agents, have been proposed for several years as an aid to diagnosis. Tanasescu et al. have described a characteristic triad in FNH: associated hypervascularization, normal uptake of colloids and accumulation of hepatobiliary tracer (*4*). However, the prevalence of this triad has not been defined in a large series of pathologically proven FNH. Moreover, a large number of cases of FNH with increased (*5–10*) or decreased (*5,6,10–11*) colloid uptake have indeed been reported. Among the few published cases of FNH studied with hepatobiliary tracers, some exhibited a decreased (*12*) or normal accumulation of the tracer (*13*). A complete analysis of the results is difficult because of the different technical conditions that have been used. These discrepancies led us to study a homogeneous series of 14 patients with 25 pathologically proven FNH tumors using hepatobiliary and colloid tracers in standardized technical conditions.

MATERIAL AND METHODS

The study was conducted from January 1990 to June 1992 and included 14 patients with FNH. All were women (age 22 to 49 yr) who had used oral contraceptives. Nine were asymptomatic. Five presented with pain in the right hypochondrium. Three had a palpable left liver lobe tumor. No patient had cholestasis, as judged on a normal level of alcalin phosphatases. All patients were referred to surgery. Twenty-five tumoral sites were found (Table 1). Six patients had multiple tumoral sites.

All tumors were diagnosed as FNH. Pathological examinations were made on resected specimens (15 tumors) or surgical biopsies (10 tumors). The resected tumors were well circumscribed but uncapsulated. A central stellate scar was observed in most cases, with radiating fibrous septa dividing the lesion into nodules. Histological examination of the resection specimens and/or of the biopsies showed that: (1) the central scar contained one or more arteries; (2) the cholangiolar proliferation was marked within and at the periphery of the fibrous septa; (3) these septa separated hyperplastic nodules from normal appearing hepatocytes. Changes suggesting tumoral compression have systematically been searched in the nontumoral liver at the vicinity of the FNH on the 15 resected tumors. These changes consisted of sinusoidal dilatation and/or cholangiolar proliferation associated with mild polymorphous inflammatory infiltration of the small portal tracts as previously described (*14*). Among the 15 resected tumors, 4 presented no compression signs, 8 presented a discrete sinusoidal dilatation, 1 presented a discrete sinusoidal dilatation and a discrete cholangiolar proliferation of the portal spaces and 2 tumors were enucleated without normal liver at the periphery.

Preoperative examinations performed on all patients included radionuclide scans and other imaging modalities (US, CT and MRI).

Two radionuclide scans were performed on every patient within a 48-hr interval. First, a hepatobiliary scan with trimethyl

Received Mar. 4, 1993; revision accepted Aug. 5, 1993.

For correspondence or reprints contact: Michel Meignan, MD, Hôpital Henri Mondor, Service de médecine nucléaire, 51, avenue du Maréchal de Lattre de Tassigny, 94010 Créteil, France.

TABLE 1
Size, Location and Imaging Characteristics of FNH Tumors

Patient no.	Tumor size (cm) and location*	TBIDA scan: Hypervascularity	TBIDA scan: Time of detectability (min)	Colloid scan (activity)	US†	CT‡	MRI‡	Discrete sinusoidal dilatation**
1	(10) III	present	22	Hypo	Iso	+	+	absent
2	(5) IV	present	27	Hypo	Iso	−	+	present
3	(4.5) VII	present	35	Iso	Hyper	+	+	present
	(1.5) III	absent	18	Iso	nd	nd	nd	present
4	(8) VI, VII, VIII	present	30-D	Hypo	Hypo	+	+	B
5	(4) III	present	30	Hypo	Iso	+	+	present
	(1) IV	absent	nd	Iso	Iso	+	+	B
6	(5) I, VIII	present	50	Hypo	Iso	+	+	B
7	(5) VII	absent	30-D	Iso-D	Hyper	+	+	B
	(3) V	absent	25	Iso	nd	−	+	present
	(10) LL	present	20	Iso	Iso	+	+	present
8	(8) VII	present	38	Iso	Hyper	−	−	B
	(4) IV	present	38	Iso	nd	−	+	E
	(1) VIII	absent	40	Iso	nd	nd	nd	B
	(10) I	present	38	Iso	Hyper	+	−	B
9	(5) IV	present	33	Iso	Iso	−	+	B
	(2) V	present	nd	Iso	nd	nd	nd	E
10	(5) III	present	35	Hypo	Hypo	+	+	absent
11	(7) III	present	28	Iso	Hypo	+	−	absent
12	(3) VIII	present	33	Hypo	Iso	+	+	B
	(1.5) VII	absent	60	Iso	Hypo	−	+	present
	(5) II	present	27	Hypo	nd	nd	nd	present
	(3) III	present	27	Iso	Iso	+	+	present
13	(8) III	present	30-D	Iso-D	Iso	+	+	absent
14	(4) IV	present	30	Hypo	Hypo	+	+	B

*Hepatic segments involved by the tumor; nd = not detected; LL = left lobe.
†US: echogenicity. ‡CT and ‡MRI: (+) criteria for FNH are present; (−) 1 or more criteria are missing.
**At the vicinity of the tumor; E = tumors enucleated without normal liver parenchyma; D = doughnut pattern observed; B = FNH diagnosis performed only on surgical biopsies.

bromo-imino-diacetic acid (TBIDA) labeled with ^{99m}Tc and second, a scan with rhenium colloid labeled with ^{99m}Tc. The hepatobiliary scan was obtained immediately after bolus intravenous injection of 180 MBq ^{99m}Tc-TBIDA (TCK22, Oris, France). The patient laid supine and images were obtained with a large field of view gamma camera equipped with a low-energy, all-purpose collimator and linked to a minicomputer (Sopha Medical—Simis System, France). A dynamic series of analog and digital images (20 one-second images and 60 two-second images) were first acquired in the anterior view. This dynamic series was followed by static 100-sec analog and digital images obtained for 1 hr in the same view. Posterior, left anterior oblique, right anterior oblique and right lateral 100-sec images were then obtained. Four hours later, anterior and posterior images were repeated with additional views if required. A minimum number of 1000 kcts per scan was achieved. Scans were displayed on 3M film (CRT 7, Trimatic 100 NIF, 8 × 10 in). Overexposed views were taken if necessary to better visualize tumors not seen on standard exposures. Thirteen patients ingested a standard fat meal 1 hr after the injection of TBIDA in order to increase biliary pressure.

Colloid liver scanning was performed 48 hr later using 180 MBq of ^{99m}Tc-rhenium sulfur colloid (TCK1, Oris, France). Anterior, posterior, oblique and lateral 800 kcts views were obtained 15 min after injection. These scans were obtained and read without knowledge of the other preoperative imaging modalities.

In all cases, adjacent axial CT scans 8 or 10 mm thick were obtained before and after intravenous administration of contrast medium in the plane of the lesion. The diagnosis of FNH by CT scans was made with classically used criteria, i.e., arterial enhancement, central stellate and hypodense areas.

MRI was performed with a 1.5 T magnet (Magnetom SP 63; Siemens) using a TurboFLASH (fast low-angle shot) sequence combined with bolus administration of gadolinium tetraazacyclododecanetetraacetic acid (DOTA), spin-echo T2-weighted sequences and postcontrast T1-weighted sequences according to a previously published protocol (*2*). The criteria used for diagnosis of FNH with MRI were: hyperintense central stellate area on T2-weighted images; hypointense central stellate area on unenhanced T1-weighted images; arterial enhancement; and accumulation of contrast agent within the central area on delayed T1-weighted images (*2*). Changes suggesting tumoral compression or edema have systematically been searched in the liver surrounding the tumor.

TBIDA kinetics in the tumor were compared to those of normal liver. We computed the time-activity curves of the tumor and the upper left or right liver lobe. From these fitted curves, the respective TBIDA excretion half-times were derived. For statistical reasons, these parameters were only computed in patients with large (>5 cm) and unique tumors sparing a large region of normal liver. An index for estimating relative size of the tumor and the liver was obtained as follows:

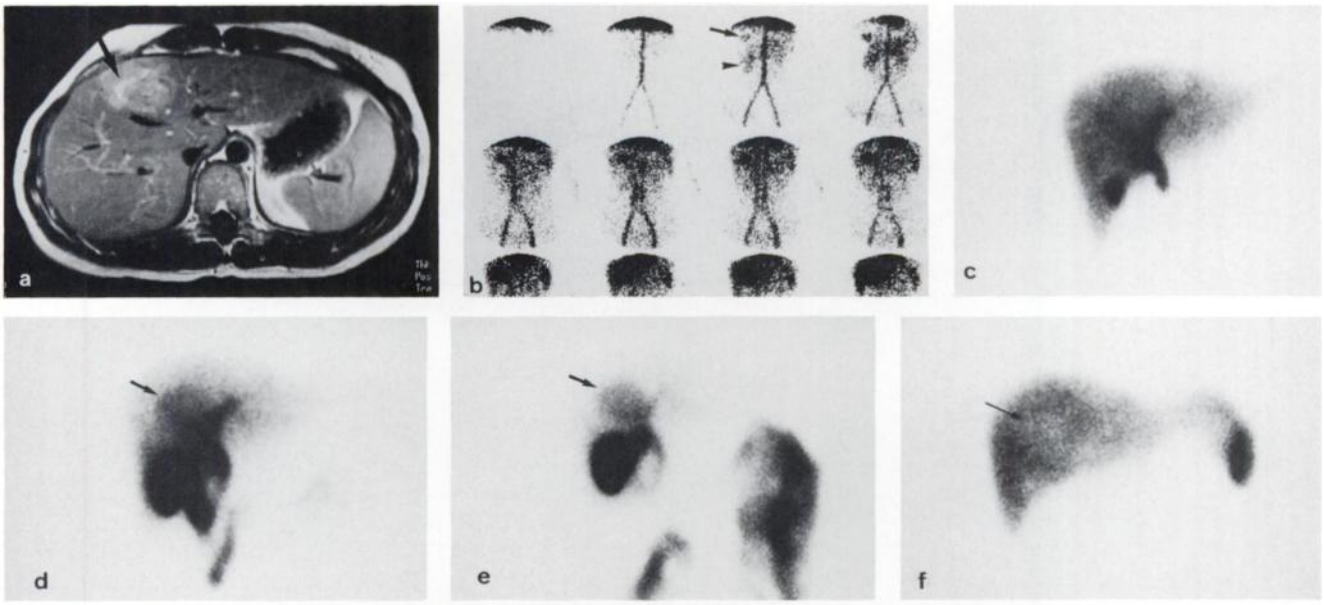

FIGURE 1. Patient 2. (a) MRI study; axial T1 weighted image obtained 4 min after injection of paramagnetic contrast agent: A 5-cm mass is visible in the right lobe of the liver with a hyperintense central scar (arrow). (b) TBIDA angiography; 1-sec images. An early vascular activity (arrow) is demonstrated in the right lobe of the liver over the renal vascular activity area (arrow head). (c) TBIDA scan at 10 min. The uptake is rather homogeneous throughout the liver. (d) TBIDA scan at 35 min. A hot spot of hyperactivity appeared in the right lobe over the gallbladder (arrow). (e) Overexposed TBIDA scan at 60 min where the hot spot is obvious (arrow) but the normal liver has already cleared the tracer. (f) Colloid liver scan. A defect is noted in the quadrate lobe (arrow). In the inferior part of the liver's right lobe, a region of the gallbladder corresponds to a discrete hypoactivity area.

1. On MRI axial images, the maximum diameter of the liver and the maximum transverse diameter of the tumor were measured with a slide rule and a tumor-to-liver ratio was computed.
2. On TBIDA anterior views, tumor-to-liver ratios were obtained by measuring the maximum liver diameter on 10-min films (*15*), and tumor diameter was obtained from 60-min images. These measurements were always performed by two observers (HB, MM).

The obtained values were compared using the t-test for paired data. A least squares method was used for regression analysis.

RESULTS

Hepatobiliary Scan

On the perfusion phase of the study, a focus of hyperactivity was observed in 76% of the tumoral sites (Figs. 1 and 2). Six tumors did not exhibit increased vascularization in the dynamic study (Table 1). Four of the tumors were small in diameter and one was larger (Table 1). Another was located in the posterior part of a liver segment.

During the first 10 min, radioactivity was relatively uniform in the liver in all patients (Figs. 1–3). By contrast,

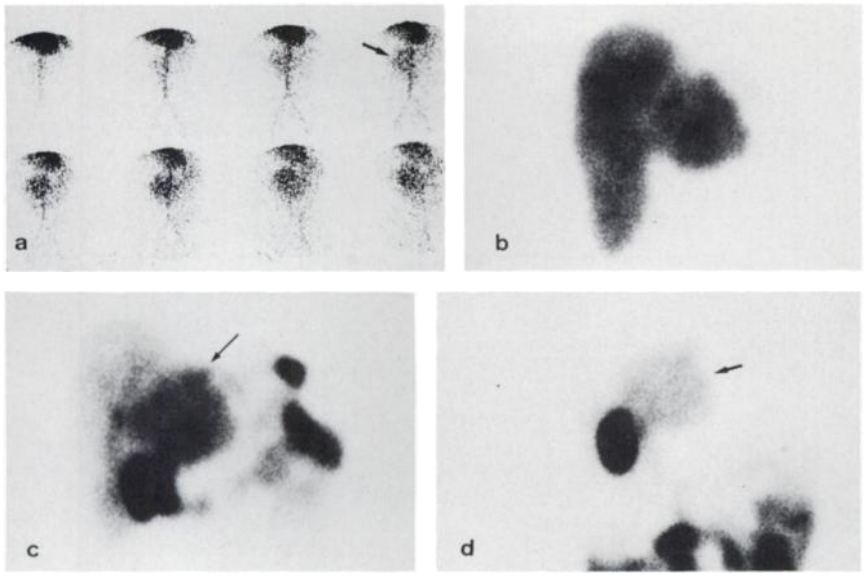

FIGURE 2. Patient 1. (a) TBIDA angiography; 1-sec images. An early vascular activity appears in the left lobe (arrow). (b) TBIDA scan at 10 min; the uptake of the tracer is practically homogeneous in the left and the right lobes. (c) TBIDA scan at 30 min. The left lobe tumor appeared as a hot spot of hyperactivity relatively to the normal liver (arrow). (d) Overexposed TBIDA scan at 60 min; a hot spot of activity is observed in the region of the huge tumor (arrow).

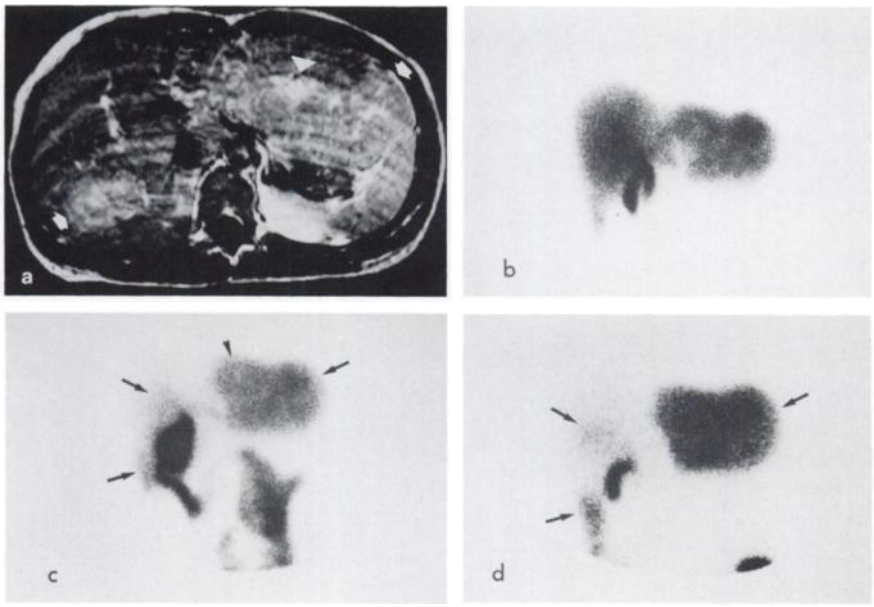

FIGURE 3. Patient 7. (a) MRI study. Axial T1-weighted image obtained 4 min after injection of paramagnetic contrast agent. Enhancement of a huge left liver lesion (10 cm) (arrow) is clearly visible with a hyperintense scar (arrowhead) corresponding to accumulation of paramagnetic agent. A second smaller lesion is also visible in the right lobe (arrow). (b) TBIDA scan at 10 min. A relatively homogeneous activity is noted in the liver. (c) Overexposed TBIDA scan at 35 min. The three lesions of the liver are noted as hot spots of hyperactivity in the left lobe and in the right lobe relatively to the normal liver (arrows). A doughnut pattern constituted by a rim of activity surrounding a focal defect is observed in the left lobe (arrowhead). (d) Overexposed TBIDA scan at 4 hr. The three lesions are yet present as hot spots of hyperactivity in left and right lobes (arrows).

during the clearance phase, 23/25 tumors demonstrated tracer retention, resulting in hyperactivity relative to the normal liver. Fifty percent of the tumors were detectable relatively early, during the first half-hour (Figs. 1 and 2). Other tumors were detected later, up to 1 hr postinjection.

Overall tumor detectability was 92%. The tumor was better defined with time as the normal liver cleared the tracer. Thus, progressively increased contrast was observed between the tumor and the liver. At 50–60 min, the tumor appeared as an isolated hot spot of radioactivity (Figs. 1–3). In three tumors, a "doughnut" pattern was observed in the radioactivity surrounding a focal defect (Fig. 3). Two tumors did not exhibit this hot spot even on the 4-hr views; one of them measured 1 cm in diameter and was located in the quadrate lobe close to the gallbladder, while the other one measured 2 cm in diameter and was located in segment V. However, these tumors occurred in patients who had other FNH lesions that exhibited high TBIDA uptake. Therefore, in all patients having one or multiple FNH, a typical hot spot was always observed in at least one tumor. In nine patients, gallbladder excretion was completed after consuming the fat meal used in this study. In four patients, increased radioactivity was still observed in the gallbladder 4 hr later.

The mean excretion half-times from tumor and normal liver presented in Table 2 showed that the excretion tumor half-time is significantly longer than half-time excretion of normal liver, which is in accordance with previous results (*15,16*) ($p < 0.01$). Half-time values were not calculated in one case because the patient moved during the examination.

Colloid Liver Scan

Sixty-four percent of the tumors exhibited normal uptake and no increased uptake was observed. Thirty-six percent of the tumors were detectable by the presence of a focal defect. A doughnut pattern was observed in two tumors.

US, CT and MRI

US, CT and MRI results are presented in Table 1. Typical features observed in FNH with MRI are shown in Figures 1 and 3. No signs of edema or compression were noted in normal liver close to the tumor with MRI. There was no significant difference between the mean tumor-to-liver ratios measured with MRI or TBIDA scanning. There was a high correlation ($r = 0.99$) between these two estimates (Fig. 4). Tumor detectability for these various techniques is illustrated by Figure 5.

DISCUSSION

Our data show that tumors appear as foci of hypervascularity in the perfusion phase followed by relatively normal uptake (initial 10 min) and as hot spots due to the retention of hepatobiliary tracer during the clearance phase on hepatobiliary scans. These findings suggest that liver cells involved in FNH maintained their normal uptake mechanisms but seem to have abnormal secretion and ex-

TABLE 2
Excretion Half-Life in Regions of Interest from Tumor and Normal Liver

Patient no.	$T_{1/2}$ tumor (min)	$T_{1/2}$ URL or ULL (min)
1	42.79	11.53
2	31.84	17.63
4	34.66	23.74
6	25.96	21.31
10	49.10	16.73
11	46.80	20.86
13	47.60	14.04
Mean ± s.d.	39.82 ± 9.00	17.97 ± 1.62

URL = upper right lobe; ULL = upper left lobe; $T_{1/2}$ = excretion half-life time in minutes.

cretion functions (*15,16*). The majority of the hot spots were detectable early in the clearance phase, whereas others appeared up to 60 min later (Table 1). These differences in the range of appearance times for hot spots probably depend on the relative clearance times of the tumor and the normal liver, thus resulting in different contrast qualities (Table 2). This phenomenon appears to be independent of tumor size (Table 1).

The hot spot is probably related to tumor function and not to poor drainage of the normal liver. No patients presented with biological cholestasis. No signs of compression or edema were detected on MR images in the surrounding tissue. Pathological examination revealed no evident signs of compression. Moreover, tumor-to-liver ratios measured with TBIDA on the basis of hot spots correlated with measurements made on MR images (Fig. 4).

Results from a previously published report (*15*) of eight cases with pathologically proven FNH studied with various hepatobiliary tracers in the same class of iminodiacetic acid organic anions (*15*), such as diethyl-IDA (DIIDA), pbutyl-IDA (PBIDA) and diisopropyl-IDA (DISIDA), are conflicting. In six of these cases, the pattern of hyperactivity was the same as in our series. A hot spot was found in three patients studied with DISIDA (*4,17*), in one patient with PBIDA (*18*) and two patients with DIIDA (*12*). In contrast, normal uptake was noted in one patient studied with DIIDA (*13*) and a focal defect was found in the region of the tumor in one patient studied with DIIDA (*12*). These differences may be related to: different behaviors of each tracer with regard to structural variances of the liver, different excretion half-times and to tumor pathology, or to different technical conditions during imaging.

A high proportion of fibrous components in some tumors could, for instance, explain a focal defect. Indeed the case of hypoactivity reported by Biersack (*12*) 20 and 60 min after injection showed a huge tumor presenting as an atypical angiographic pattern composed of hypovascularized and hypervascularized regions. Twenty minutes after injection, the hypovascularized region, which could correspond to fibrous tissue, exhibited decreased uptake of DIIDA, while tracer was still present in the hypervascularized region. Sixty minutes after injection, the foci of residual activity could be individualized in the tumoral region, while normal liver had already cleared the tracer. Such a fibrotic effect, which contains few or no bile ducts, on induction of hypoactivity could probably explain the doughnut pattern observed in our study.

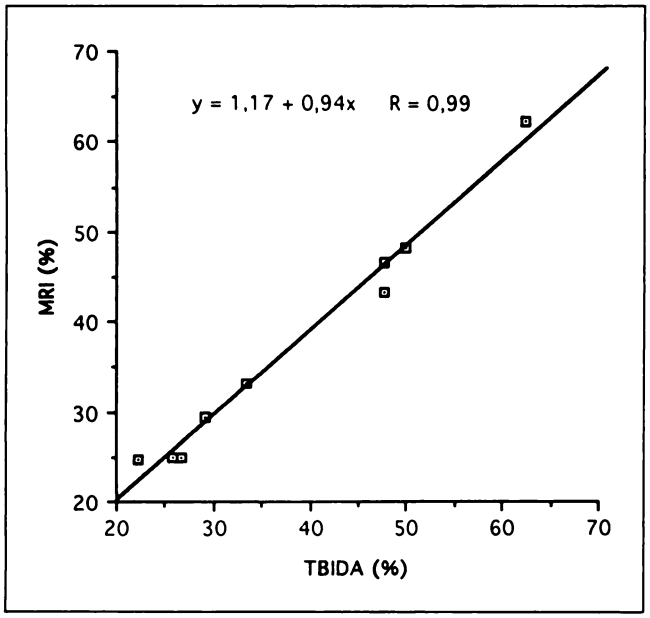

FIGURE 4. Correlation between the tumor-to-liver ratio percentages obtained on TBIDA and MRI.

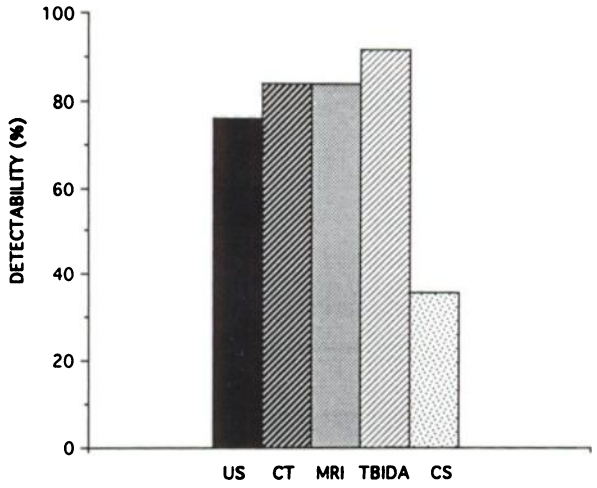

FIGURE 5. Percentage of detectability for the various imaging techniques (CS = colloid scan).

Peterfy et al. reported normal uptake in a large telangiectatic FNH (*13*). The tumor, which was imaged with DIIDA, was located in close proximity to the gallbladder which demonstrated dramatically increased activity with time.

The behavior of hepatobiliary tracers in FNH might be explained by the peculiar histological characteristics of this tumor. Our results show that hypervascularity is demonstrated during the blood transport phase in accordance with radiological findings (*2,12*). The uptake phase is relatively normal, indicating that FNH hepatocytes do not have any difficulty in concentrating IDA agents (*15,16*). The fact that FNH tissues become increasingly visible at later times, especially at 60 min, clearly demonstrates that the hepatocytes or the bile canaliculi draining these hepatocytes are at fault, hence the slow clearance of IDA from the nodule. Tumor excretion half-times are longer when compared to normal liver tissue (Table 2), thus confirming the slower clearance of IDA (*12,15–17*).

In the present study, the TBIDA scan failed to detect two FNH lesions. In one patient, the tumor was in the quadrate lobe in the region of the gallbladder. Because no gallbladder response was observed after consumption of a fatty meal, the tumor could have been masked by gallbladder hyperactivity. In the second negative case, the tumor size was small (2 cm in diameter) and the tumor was located in the center of the segment. For practical reasons, we did

not take overexposed views, but the tumor was not detectable on the digital images in spite of contrast enhancement.

In our study, the presence of a hot spot after imaging with hepatobiliary tracers occurs more frequently in FNH. This high prevalence can be explained by the functional properties of TBIDA, which has the highest clearance among hepatobiliary tumors and increases the contrast between retention zones and normal liver (*15,16*), and by improvements in detectability due to technical conditions. Late images and overexposed views are necessary for the detection of tumors with faintly retained activity. Multiple views are particularly useful. Gallbladder excretion must be stimulated to allow assessment of segments near this organ. Although we used a fatty meal in this study, we now use cholekinetic agents which produce faster excretion. Digital frame processing would probably help in image analysis when overexposed films are inconclusive, thus allowing for gallbladder subtraction or intestinal activity.

Of the triad of elements suggested by Tanasescu et al., i.e., hypervascularization, normal colloid uptake and hepatobiliary tracer retention, tracer retention on hepatobiliary scan was the most frequent sign.

Hypervascularization is undetectable in small tumors and may be masked by aortic, coeliac and renal vascular activities or missed by the use of anterior views in posterior liver tumor (Table 1, Patient 7).

The results obtained in our series with colloid scans are in accordance with previous series (Table 1). There are 67 reported cases of FNH studied with sulfur colloid in the literature. Ten scans with increased uptake (*5–10*) and 33 with normal uptake were indeed observed in the tumor (*5,6,10,19*), but 24 scans showed a focal defect (*5,6,10,11*). The presence of a focal defect or normal uptake depends on the size and the number of Kupffer cells present in the lesion (*20*). The existence of large amounts of fibrotic cells might also explain the focal defects. However, the reason for increased uptake has not been clearly explained. In our study, hepatobiliary tracer retention was observed in 92% of FNH. In contrast, MRI and CT scans showed only an 84% detectability (Fig. 5).

However, the specificity of the hot spot was not determined in this study. Such hot spots have been described mainly in FNH and hepatocellularcarcinoma (*21,22*). It must be stressed, however, that such carcinomas occur in completely different diagnostic circumstances. Belfer et al. reported one case of liver adenoma with a hot spot (*23*), but there is not enough histopathological documentation to prove that this was a true case of liver cell adenoma.

A large prospective study would be necessary to precisely define the diagnostic value of the pattern of hepatobiliary tracer distribution we have observed in FNH. Obviously, such a study should include other types of tumors such as liver adenomas. Since liver adenoma is now infrequently encountered (possibly due to low dosage of estrogens in contraceptive pills), such a study should be multicentric. Nevertheless, from our data and those from the literature, hepatobiliary scans that demonstrate hot spots in the region of the tumor, seem to be an useful tool when combined with other imaging techniques in the diagnosis of FNH.

ACKNOWLEDGMENT

This work was presented at the 39th Annual Meeting of the Society of Nuclear Medicine, Los Angeles, CA, June, 1992.

REFERENCES

1. Butron Vila MM, Haot J, Desmet VJ. Cholestatic features in focal nodular hyperplasia of the liver. *Liver* 1984;4:387–395.
2. Mathieu D, Rahmouni A, Anglade MC, et al. Focal nodular hyperplasia of the liver: assessment with contrast-enhanced turboFLASH MR imaging. *Radiology* 1991;180:25–30.
3. Vilgrain V, Fléjou JF, Arrivé L, et al. Focal nodular hyperplasia of the liver: MR imaging and pathologic correlation in 37 patients. *Radiology* 1992;184: 699–703.
4. Tanasescu D, Brachman M, Rigby J, Yadegar J, Ramanna L, Waxman A. Scintigraphic triad in focal nodular hyperplasia. *Am J Gastroenterol* 1984; 79:61–64.
5. Salvo AF, Schiller A, Athanasoulis C, et al. Hepatoadenoma and focal nodular hyperplasia: pitfalls in radiocolloid imaging. *Radiology* 1977;125: 451–455.
6. Welch TJ, Sheedy PF, Johnson CM, Galdabini J, McKusick KA. Focal nodular hyperplasia and hepatic adenoma. Comparison of angiography, CT, US, and scintigraphy. *Radiology* 1985;156:593–595.
7. Atkinson GD, Kodroff M, Sones PJ, Gay BB. Focal nodular hyperplasia of the liver in children: a report of three new cases. *Radiology* 1980;137:171–174.
8. Piers DA, Houthoff HJ, Krom AF, Schuur KH. Hot spot liver scan in focal nodular hyperplasia. *AJR* 1980;135:1289–1292.
9. Pasquier J, Dorta T. Focal hyperfixation of radiocolloid by the liver [Letter]. *J Nucl Med* 1974;15:725.
10. Rogers JV, Mack LA, Freeny PC, Johnson ML, Sones PJ. Hepatic focal nodular hyperplasia: angiography, CT, sonography and scintigraphy. *AJR* 1981;137:983–990.
11. Jhingram SG, Mukhopadhyay AK, Ajmani SK, Johnson PC. Hepatic adenomas and focal nodular hyperplasia of the liver in young women on oral contraceptives: case reports. *J Nucl Med* 1977;18:263–266.
12. Biersack HJ, Thelen M, Torres JF, Lackner K, Winkler CG. Focal nodular hyperplasia of the liver as established by ^{99m}Tc sulfur colloid and HIDA scintigraphy. *Radiology* 1980;137:187–190.
13. Peterfy CG, Rosenthall L. Large telangiectatic focal nodular hyperplasia presenting with normal radionuclide studies. Case report. *J Nucl Med* 1990;31:2037–2039.
14. Gerber MA, Thung SN, Bodenheimer HC, Kapelman B, Schaffner F. Characteristic histologic triad in liver adjacent to metastatic neoplasm. *Liver* 1986;6:85–88.
15. Krishnamurthy S, Krishnarmurthy G. Technetium-99m iminodiacetic acid organic anions: review of biokinetics and clinical application in hepatology. *Hepatology* 1989;9:139–153.
16. Krishnamurthy S, Krishnarmurthy G. Quantitative assessment of hepatobiliary disease with Tc-99m IDA scintigraphy. In: Freeman LM, Weissmann HS, eds. *Nuclear medicine annual*. New York: Raven Press; 1988: 309–330.
17. Desai M, Kroop S, Sullivan J, Santaseri V, Zanzi I, Margouleff D. Focal nodular hyperplasia of the liver: correlation of Tc-99m DISIDA "hot spot" appearance with histopathologic findings. *Clin Nucl Med* 1989;11:814–816.
18. Hoshi H, Mihara K, Nakano T, et al. Tc-99m phytate and Tc-99m P-butyl IDA scintigraphy in focal nodular hyperplasia of the liver. *Clin Nucl Med* 1982;7:423–424.
19. McLoughlin MJ, Colapinto RF, Gilday DL, et al. Focal nodular hyperplasia of the liver; angiography and radioisotope scanning. *Radiology* 1973;107: 257–263.
20. Goodman ZD, Mikel UV, Lubbers PR, Ros PR, Langloss JM, Ishak KG. Kupffer cells in hepatocellular adenomas. *Am J Surg Pathol* 1987;11:191–196.
21. Lee VW, O'Brien MJ, Devereux DF, Morris PM, Shapiro JH. Hepatocellular carcinoma: uptake of ^{99m}Tc-IDA in primary tumor and metastasis. *AJR* 1984;143:57–61.
22. Calvet X, Pons F, Bruix J, et al. Technetium-99m-DISIDA hepatobiliary agent in diagnosis of hepatocellular carcinoma: relationship between detectability and tumor differentiation. *J Nucl Med* 1988;29:1916–1920.
23. Belfer AJ, Grijm R, Shoot JB. Hepatic adenomas: imaging with different radionuclides. *Clin Nucl Med* 1979;4:375–378.